

BOTTOMONIA UNDER EFFECT THREE INSPIRED QCD POTENTIALS IN THE FRAMEWORK OF NON-RELATIVISTIC QUARK MODEL[†]

✉ Moustafa Ismail Hapareer^{a,*}, ✉ M. Allosh^b, ✉ G.S. Hassan^a, ✉ A.M. Yasser^b

^a Physics Department, Faculty of Science, Assiut University, 71515 Assiut, Egypt

^b Physics Department, Faculty of Science, Qena, South Valley University, 83523 Qena, Egypt

*E-mail: mostafa.ismail.hapareer@science.aun.edu.eg

Received March 18, 2023; revised April 5, 2023; accepted May 18, 2023

In this paper, we have studied the spectrum of bottomonium mesons behavior under the effect of three types of potentials inspired by Quantum Chromodynamics. In addition, other properties like Hyperfine splitting behavior, and Fine splitting behavior have been studied. We used these potential models within the non-relativistic quark model to present this study. We found that our expectations are consistent with experimental data and other theoretical works as well we presented new conclusions regarding the spectrum of unseen bottomonium states for S, P, and D-wave bottomonia. And we have expected other their characteristics.

Keywords: *Hyper splitting behavior, Fine splitting behavior, bottomonia*

PACS: 12.40.Yx, 14.40.Pq, 02.60.Cb, 12.39.Jh, 14.65.Dw, 14.40.Lb, 14.80.Bn

1. INTRODUCTION

Investigation of heavy quarkonia systems like charmonium, bottomonium, and toponium, offers a clear understanding of particle physics, the standard model, and the quantification characterization of the QCD quantum chromodynamics theory [1, 2, 3, 4]. But because of the tiny lifetime for the top quark approximately equals $0.5 \times 10^{-24} s$, it is very hard to appear in nature [5]. So we can say the bottomonia are the heaviest mesons that the experiments discovered them over a long time. From that, the bottomonium family holds a substantial place in the hadronic particles and participates effectively in the inspecting of strong interactions.

The full observed bottomonium spectra are still very far from the establishing, in comparison with the theoretical calculations of spectra. Ref.[5] provides a good review of the practical history of the bottomonium states, but here we offer a brief summary. At Fermilab by the E288 Collaboration in 1977, the first bottomonia $\Upsilon(1S)$ and $\Upsilon(2S)$ plus $\Upsilon(3S)$ have been detected [6, 7]. Then $\Upsilon(4S)$ state was observed in 1984 [8]. BaBar Collaboration has observed $\eta_b(1S)$, the spin-singlet partner of the spin-triplet state $\Upsilon(1S)$, in 2008 [9]. After four years, Belle collaboration has announced the initial evidence for spin-singlet partner $\eta_b(2S)$ of the $\Upsilon(2S)$ in 2012 utilizing the transition process, $h_b(2P) \rightarrow \gamma$ [10]. In 1982 [11, 12] and 1983 [13, 14], the radiative transitions of the $\Upsilon(2S)$ and $\Upsilon(3S)$ have led to the observation of the two triplet-spin P-wave mesons $\chi_{bJ}(1P)$ and $\chi_{bJ}(2P)$ with $J = 2, 1, 0$. $h_b(1P)$ has firstly manifested in BABAR in 2011 via cascade transitions; $\Upsilon(3S) \rightarrow \pi^0 h_b(1P) \rightarrow \pi^0 \gamma \eta_b(2S)$ [15], with a mass of $9902 \pm 4 \pm 2$. Belle has not long waited to announce significant observation of the singlet spin states $h_b(2P)$ [16]. In the cascade transitions, $\Upsilon(3S) \rightarrow \chi_b(2P) \gamma \rightarrow \Upsilon(1^3D_2) \gamma \gamma \rightarrow \chi_b(1P) \gamma \gamma \gamma \rightarrow \Upsilon(1S) \gamma \gamma \gamma$, the candidate for the mesonic state; 1^3D_2 has appeared in the CLEO Collaboration in 2004 [17].

So clear, it is hard to assign the whole spectrum of bottomonia. As a part of fact, we are still at the beginning of this road. Until now many lower bottomonium states that are under the threshold of creation of the $B\bar{B}$ pair have not appeared. But the running of the Belle II [18] and upcoming colliders will open the hope door towards this challenge, and we foresee the appearance of new bottomonium states. To achieve that, we need to probe the bottomonia with many theoretical techniques that provide us with accurate expectations and inspired QCD. There are many techniques have utilized for example; the QCD sum rule [19, 20], Bethe-Salpeter [21], the Regge phenomenology [22, 23, 24, 25], the method of perturbative QCD [26], the lattice QCD [27, 28, 29], and the coupled-channel model [30, 31, 32, 33] in addition to utilizing the versions of relativistic [34, 35], relativized [36, 37, 38], semi-relativistic [39, 40], and finally the non-relativistic [41].

Our purpose in this paper is to obtain the accurate mass spectrum of bottomonia in addition to the characteristics of hyperfine splitting behavior and fine splitting behavior. We suggest applying three QCD-inspired potentials, the first one is the simplest. For more accurate results, we use the second one, which takes into account the spin-spin interactions between quarks. Here appears the hyperfine splitting behavior. To obtain the best potential, which is more sophisticated and more accurate, we apply the third one, which

[†] *Cite as:* Moustafa Ismail Hapareer, M. Allosh, G.S. Hassan, A.M. Yasser, East Eur. J. Phys. 2, 348 (2023), <https://doi.org/10.26565/2312-4334-2023-2-41>

includes spin-orbit interactions and tensor interactions, and here the fine-splitting behavior appears, and the results become more accurate. The theoretical frame for this work is in the next section, while we offer our findings and discussion in section 3. Our conclusions appear in the last section.

2. THE THEORETICAL FRAME

We adopt the non-relativistic approximation, which includes the Hamiltonian that rules the dynamics of mesons, consisting of the kinetic energy part \mathcal{T} and the potential energy part \mathcal{V} which considers the phenomenological interactions of the constituent quarks. We can write the Hamiltonian operator $\hat{\mathcal{H}}$ as:

$$\hat{\mathcal{H}}_{nr} = \hat{\mathcal{T}}_{nr} + \hat{\mathcal{V}}. \tag{1}$$

We can express the wave functions of mesons as the eigenfunctions in the Schrödinger equation as follows:

$$\hat{\mathcal{H}}_{nr}\psi = \mathcal{E}\psi. \tag{2}$$

2.1. The Kinetic Energy of Bottomonia

We can treat the bottomonium mass center of motion as the non-relativistic kinetic energy. The expression of the non-relativistic kinetic energy operator is as the next [42]:

$$\hat{\mathcal{T}}_{nr} = m_b + m_{\bar{b}} + \frac{\hat{\mathcal{P}}^2}{\mu}. \tag{3}$$

The m_b and $m_{\bar{b}}$ are the masses of the bottom quark and the bottom antiquark. The μ and $\hat{\mathcal{P}}$ are the reduced mass and the relative momentum of bottomonium meson, respectively. The constituent quark mass is used to provide us with suitable calculations of bottomonium properties that could be performed. We can compare the findings to the experimental data [43] to appear how our models work.

2.2. The Potential Models

From a time the first detection of the charmonium states in 1974, the first system of quark and antiquark, it became prototypical of the exotic positronium atom e^+e^- for meson spectroscopy [44, 45, 46]. There is a similarity between them roughly [1]. So the initial attempt started to improve positronium-like potential, to obtain a fine static potential of quarkonium, which is known as a vector color coulomb-like potential. The improved color coulomb-like potential depends on QCD spirit. In this potential, the effectiveness of quark interaction is in the short distances [47, 48]. According to the rules of quantum chromodynamics (QCD) theory, the behavior of short distance has dominated via one-gluon exchange (OGE) interaction[49, 1]. Hence the color coulomb-like potential takes the following formula:

$$\mathcal{V}_{coulomb-like}(r) = \frac{-4}{3} \frac{\alpha_s}{r} \tag{4}$$

where α_s and $\frac{-4}{3}$ are the running strong coupling constant and the color factor, respectively. From the phenomenological side, we must consider the quark confinement at the long ranges[36, 42], where one of the significant properties of strong interactions is confinement, which is generally acknowledged. From QCD rules, the confining potential increases with increasing the inter-quark distance[50, 1]. So we can write the confinement potential as:

$$\mathcal{V}_{conf}(r) = br. \tag{5}$$

From the previous, we can obtain the conventional potential, which collects the vector color Coulomb-like potential as in Eq.4 and the scalar linear potential as in Eq.5. This is the first suggested potential that we can write as:

$$\mathcal{V}_I(r) = \frac{-4}{3} \frac{\alpha_s}{r} + br. \tag{6}$$

We will investigate $b\bar{b}$ system spectra under the effect of this potential as a minimal potential model, as shown in Table 2; column 4.

Here, we go ahead a step toward the front to consider the spin-spin interactions between $b\bar{b}$ systems, which takes the following relation:

$$\mathcal{V}_{SS}(r) = \frac{32\pi\alpha_s}{9m_b m_{\bar{b}}} \delta_\sigma(r) \mathbf{S}_b \cdot \mathbf{S}_{\bar{b}} \tag{7}$$

where

$$\delta_\sigma(r) = (\sigma/\sqrt{\pi})^3 e^{-\sigma^2 r^2}. \tag{8}$$

When we add Eq.7 to Eq.6, we acquire the second potential that takes the following form:

$$\mathcal{V}_{II}(r) = \frac{-4}{3} \frac{\alpha_s}{r} + br + \frac{32\pi\alpha_s}{9m_b m_{\bar{b}}} \delta_\sigma(r) \mathbf{S}_b \cdot \mathbf{S}_{\bar{b}}, \tag{9}$$

where

$$\langle SM_s | \mathbf{S}_b \mathbf{S}_{\bar{b}} | SM_s \rangle = \frac{S(S-1)}{2} - \frac{3}{4} \tag{10}$$

as S is the total spin of the meson [51]. The second potential considers the hyperfine behavior that arises due to spin-spin interaction between quarks, so it differentiates between the triplet spin states and singlet spin states. Now we take into account two significant parts spin-orbit interactions and tensor interactions. They have the next formulas[52]:

$$\mathcal{V}_{SL}(r) = \frac{1}{2m_b^2 r} (3\mathcal{V}'_V(r) - \mathcal{V}'_S(r)) \mathbf{L} \cdot \mathbf{S}, \tag{11}$$

and

$$\mathcal{V}_T(r) = \frac{1}{12m_b^2} \left(\frac{1}{r} \mathcal{V}'_V(r) - \mathcal{V}''_V(r) \right) \mathbf{T} \tag{12}$$

where the spin-orbit matrix elements of the $\mathbf{L} \cdot \mathbf{S}$ operator is determined by

$$\langle \mathbf{L} \cdot \mathbf{S} \rangle = \frac{J(J+1)}{2} - \frac{L(L+1)}{2} - \frac{S(S+1)}{2}, \tag{13}$$

where L and J are orbital angular momentum and total angular momentum quantum numbers. This operator has a diagonal base $|J, L, S\rangle$, and T represents the tensor operator [53]:

$$\mathbf{T} = \mathbf{S}_q \cdot \hat{r} \mathbf{S}_{\bar{q}} \cdot \hat{r} - \frac{1}{3} \mathbf{S}_q \cdot \mathbf{S}_{\bar{q}} \tag{14}$$

From the equations (9,11,12), we can write the third potential as follows:

$$\mathcal{V}_{III}(r) = \frac{-4}{3} \frac{\alpha_s}{r} + br + \frac{32\pi\alpha_s}{9m_b m_{\bar{b}}} \delta_\sigma(r) \mathbf{S}_b \cdot \mathbf{S}_{\bar{b}} + \mathcal{V}_{SL}(r) + \mathcal{V}_T(r). \tag{15}$$

This potential considers fine splitting behavior due to taking into account the spin-orbit and the tensor interactions in addition to the hyperfine splitting behavior due to spin-spin interaction.

We have determined the utilized parameters in these potentials by fitting the corresponding spectrum of bottomonium states for each different potential, as in Table 1. We can have high expectations concerning the bottomonia spectrum ($b\bar{b}$), as shown in Table 2 due to, these modified parameters tabulated in Table 1.

Table 1. The modified parameters were utilized in three potentials to obtain the masses of $b\bar{b}$ -bottomonium states

Model Parameters	The potentials in the (NRQM)		
	\mathcal{V}_I	\mathcal{V}_{II}	\mathcal{V}_{III}
$m_b = m_{\bar{b}}$ GeV	4.7836	4.7916	4.8087
α_s	0.3811	0.3981	0.4040
b (GeV) ²	0.1625	0.1671	0.1620
σ GeV	—	2.8241	2.2927

3. RESULTS AND DISCUSSION

In this paper, we remedied Schrodinger’s equation using the matrix method to obtain its numerical solution. Using the previous three potentials, the bottomonium mesons’ characteristics are probed in the frame of the non-relativistic kinetic energy. We have obtained Hamiltonian values for the $nS(n \leq 4)$, $nP(n \leq 3)$, and $nD(n \leq 3)$ bottomonium states with the spectroscopic notation $n^{2S+1}L_J$. The mass and other characteristics are introduced in Tables (2 : 4).

3.1. The Mass Spectrum of Bottomonium Mesons

We investigated the spectrum of S, P, and D-Wave bottomonium mesons under the influence of three potentials. This study includes thirty-six seen and unseen meson states. Fitting with seventeen mesonic states in the last update of data, due to it yields new parameters in each potential to get the best new theoretical bottomonium spectra in three QCD-inspired potentials types, as shown in Table 1. These newly yielded theoretical spectra were compared with the current experimental data [43] and compared to other works for calculated spectra [54, 55, 56].

The χ^2 values for the expectations of the three potential types are (0.0010), (0.0005), and (0.0002), respectively. So, one observes that the first potential type provides us an agreement with the experiment, although it is a blind model concerning the multiplets of bottomonium states that own the same orbital angular momentum L quantum number with different spin quantum number S and different total angular momentum J as in column 4 of Table 2. When we go ahead a step toward more accuracy, we find the second potential type that supplies us with more accuracy than the first one, but one notices it is a blind relative to the multiplets that own the same orbital angular momentum L quantum number, with a different total angular momentum quantum number J, as seen in column 5 of Table 2. Now we continue ahead another step toward more accuracy, and we have found that the third type of potential has achieved the most accuracy concerning these potentials, in addition, this potential provides us with the ability to distinguish between the multiplets of bottomonia that own the same quantum number L and with different quantum numbers S and J, as shown in Table 2 column 6.

The masses of bottomonia are plotted in Fig.1 and Fig.2 with the principle quantum number (n). Where the masses are extracted within the third potential type; based on its parameters which are in Table 1. The figures illustrate the masses of S, P, and D-wave states with triplet spin (in Fig.1) and singlet spin (in Fig.2) with various values of J. The graphs demonstrate that the mass spectra increase along with increasing the principle quantum number (n). Here, we find (n) has a strong influence on the S, P, and D-wave bottomonia masses when particles have the same S and J quantum numbers.

Figures 6 and 7 illustrate the theoretical masses of S, P-wave bottomonium states ($\Upsilon(nS)$ and $\eta(nS)$) and ($\chi(nS)$ and $h(nS)$), respectively. They provide us with a comparison between the practical data and the theoretical expectations using the third potential, tabulated in Table 2. we find a good consistency between them and observe a tiny distinction between them.

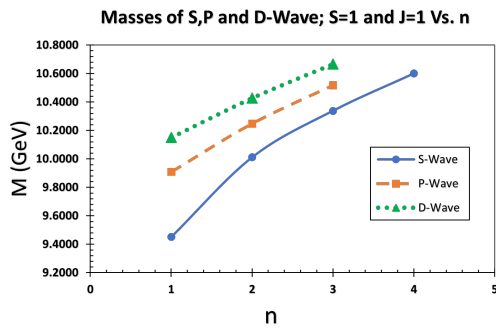
The other studies for the bottomonium spectra employed a variety of models, including the variational method with a single Gaussian trial wavefunction in a Cornell potential model in the relativistic Quark Model framework used by (Virendrasinh Kher et al.) [54]. While (B. Chen et al.) utilized the RFT model[55], meanwhile the Non-Relativistic with Screened Potential Model is applied by (W.J. Deng et al.) [56]. And (M. Wurtz et al.) use the LATTICE Field Theory estimations [29]. We find from Table. 2 that the three potentials to which we applied them agree in general in the most estimations with these models, but the third one owns the most agreement with the most states.

3.2. Hyperfine Splitting Behavior $\Delta M_{Hyp.Sp.}$

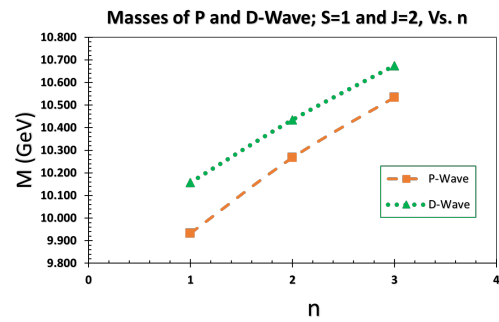
The hyperfine splitting force plays an influential role in the calculations of the mass of bottomonia. So, we have to take it into account. This force started with the appearance through the second potential, so the second potential provides us with more accurate calculations for masses than the first potential, as evident in column 5 of Table 2. However, its accuracy is further improved in the third potential to supply us with more accurate calculations, as extremely evident in column 6 of Table 2. We notice that the difference between the multiplets decreases by increasing (n) for S-wave bottomonia; the same thing concerning P-wave, but in the S-wave bottomonia the triplet spin particles have greater mass than the singlet spin particles. While the opposite happens for the P-wave bottomonia, the spectrum mass of singlet spin particles is heaviest than triplet spin particles. While in the D-wave bottomonia, the mass difference is constant between triplet, and singlet spin particles, and compared to the singlet spin particles, the triplet spin particles are heavier. Fig. 3 shows the relation between the hyperfine splitting mass and the quantum number (n) in comparison with experimental data for the S-wave in a graph (a) and also for the P-wave in graph (b) according to the third potential.

3.3. Fine Splitting Behavior $\Delta M_{F.S.}$

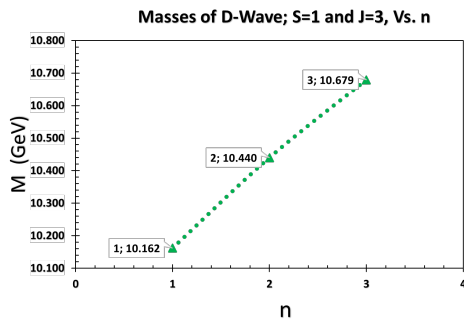
The role of fine splitting force, which appears in the third potential is very significant for estimations of the masses of bottomonium mesons. That matter makes us enter this force in our calculations of mass spectra, not only in the bottomonium spectrum but in all hadronic spectra. Consequently, we find the mass estimations are the most accurate. Also, it can distinguish between the multiplets that have the same L and S, but they have various J because of spin-orbit force and tensor force, as is very clear in Table 2; column 6. Now we find the $1^3P_1-1^3P_0$ is the dominant partial splitting where it is of ($\cong 59\%$) relative to total splitting concerning the 1P-level. Also, the $2^3P_1-2^3P_0$ takes ($\cong 55\%$) to be the dominant partial splitting relative to the 2P-level.



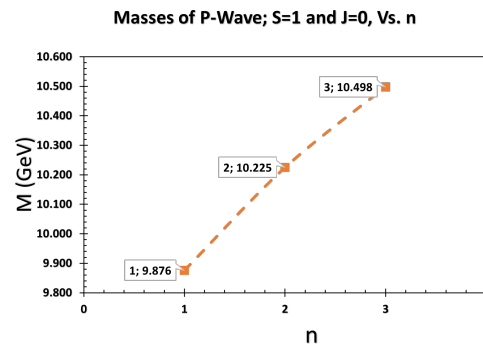
(a) The masses of S, P, and D states for J=1.



(b) The masses of P and D states for J=2.

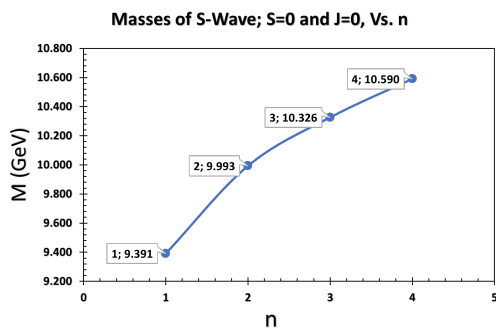


(c) The masses of D states for J=3.

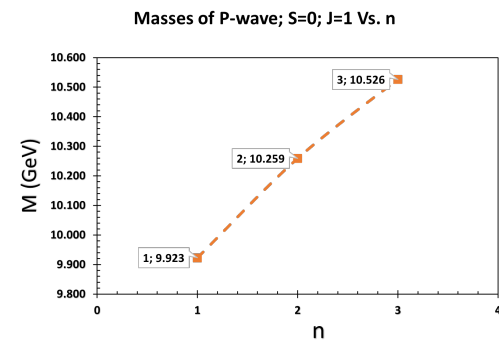


(d) The masses of P states for J=0.

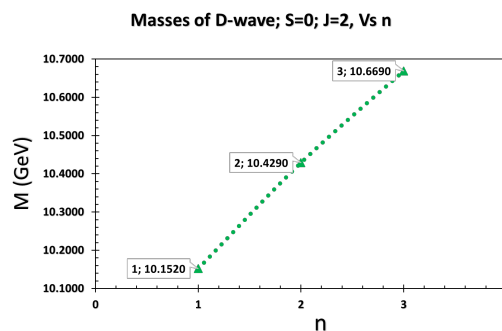
Figure 1. The Masses of S, P, and D states for QCD-inspired \mathcal{V}_{III} , which have spin one and various total angular momentum J versus n quantum number



(a) The masses of S states for J=0.



(b) The masses of P states for J=1.

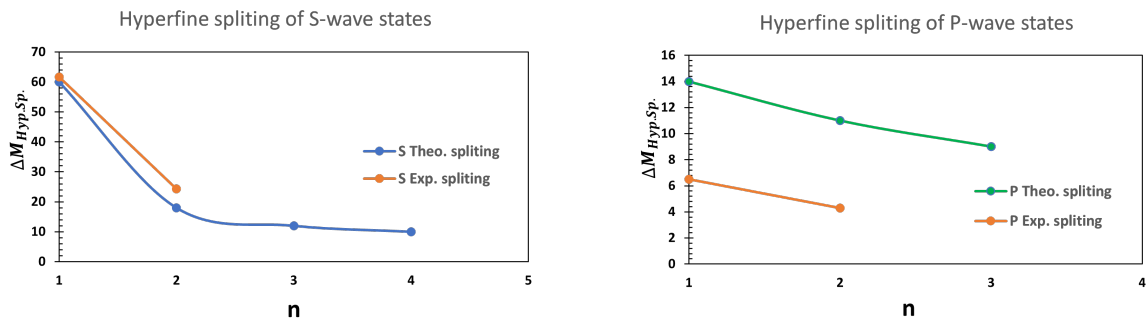


(c) The masses of D states for J=2.

Figure 2. The Masses of S, P, and D states for QCD-inspired \mathcal{V}_{III} , which have spin zero and various total angular momentum states J versus n quantum number

Table 2. Theoretical spectra of $b\bar{b}$ states in GeV under the influence of three QCD-inspired potentials compared with experimental data [43] and with theoretical results of Refs. [[54], [55], [56], [29]].

state	name	EXP.Mass [43]	Theoretical masses						
			\mathcal{V}_I	\mathcal{V}_{II}	\mathcal{V}_{III}	[54]	[55]	[56]	[29]
1 3S_1	$\Upsilon(1S)$	9.4603 ± 0.26	9.4353	9.4383	9.4510	9.4630	–	9.4600	9.4600
1 1S_0	$\eta_b(1S)$	9.3987 ± 2.0	9.4353	9.3633	9.3910	9.4230	–	9.3900	9.4020
2 3S_1	$\Upsilon(2S)$	10.0233 ± 0.31	9.9804	9.9974	10.0110	10.0010	10.0230	10.0150	10.0200
2 1S_0	$\eta_b(2S)$	9.9990 ± 4.0	9.9804	9.9722	9.9930	9.9830	9.9990	9.9900	9.9980
3 3S_1	$\Upsilon(3S)$	10.3552 ± 0.5	10.3042	10.3285	10.3380	10.3540	10.3570	10.3430	10.3340
3 1S_0	$\eta_b(3S)$		10.3042	10.3112	10.3260	10.3420	10.3370	10.3260	10.3140
4 3S_1	$\Upsilon(4S)$	10.5794 ± 1.2	10.5649	10.5949	10.6000	10.6500	10.6370	10.5970	–
4 1S_0	$\eta_b(4S)$		10.5649	10.5809	10.5900	10.6380	10.6270	10.5840	–
1 3P_2	$\chi_{b2}(1P)$	9.9122 ± 0.26 ± 0.31	9.8901	9.9012	9.9320	9.9070	9.9110	9.9210	9.9130
1 3P_1	$\chi_{b1}(1P)$	9.8928 ± 0.26 ± 0.31	9.8901	9.9012	9.9090	9.8940	9.8930	9.9030	9.8930
1 3P_0	$\chi_{b0}(1P)$	9.8594 ± 0.42 ± 0.31	9.8901	9.9012	9.8760	9.8740	9.8540	9.8640	9.8650
1 1P_1	$h_b(1P)$	9.8993 ± 0.8	9.8901	9.8990	9.9230	9.8990	9.8990	9.9090	9.9000
2 3P_2	$\chi_{b2}(2P)$	10.2686 ± 0.22 ± 0.50	10.2230	10.2433	10.2670	10.2740	10.2680	10.2640	10.2270
2 3P_1	$\chi_{b1}(2P)$	10.2555 ± 0.22 ± 0.50	10.2230	10.2433	10.2480	10.2650	10.2590	10.2490	10.2120
2 3P_0	$\chi_{b0}(2P)$	10.2325 ± 0.40 ± 0.50	10.2230	10.2433	10.2250	10.2480	10.2390	10.2200	10.1940
2 1P_1	$h_b(2P)$	10.2598 ± 1.20	10.2230	10.2409	10.2590	10.2680	10.2620	10.2540	10.2190
3 3P_2	$\chi_{b2}(3P)$	10524.0 ± 0.8	10.4896	10.5162	10.5340	10.5760	10.5560	10.5280	–
3 3P_1	$\chi_{b1}(3P)$	10513.4 ± 0.7	10.4896	10.5162	10.5170	10.5670	10.5570	10.5150	–
3 3P_0	$\chi_{b0}(3P)$		10.4896	10.5162	10.4980	10.5510	10.5510	10.4900	–
3 1P_1	$h_b(3P)$		10.4896	10.5138	10.5260	10.5700	10.5560	10.5190	–
4 3P_2	$\chi_{b2}(4P)$		10.7220	10.7537	10.7667	–	10814	–	–
4 3P_1	$\chi_{b1}(4P)$		10.7220	10.7537	10.7500	–	10817	–	–
4 3P_0	$\chi_{b0}(4P)$		10.7220	10.7537	10.7342	–	10815	–	–
4 1P_1	$h_b(4P)$		10.7220	10.7512	10.7594	–	10815	–	–
1 3D_3	$\Upsilon_3(1D)$		10.1238	10.1423	10.1620	10.1500	10.1830	10.1570	10.1720
1 3D_2	$\Upsilon_2(1D)$	10.1637 ± 1.40	10.1238	10.1423	10.1570	10.1490	10.1640	10.1530	10.1610
1 3D_1	$\Upsilon_1(1D)$		10.1238	10.1423	10.1500	10.1450	10.1360	10.1460	10.1500
1 1D_2	$\eta_{b2}(1D)$		10.1238	10.1422	10.1520	10.1490	10.1670	10.1530	10.1630
2 3D_3	$\Upsilon_3(2D)$		10.3996	10.4245	10.4400	10.4660	10.4780	10.4360	10.4590
2 3D_2	$\Upsilon_2(2D)$		10.3996	10.4245	10.4340	10.4650	10.4760	10.4320	10.4010
2 3D_1	$\Upsilon_1(2D)$		10.3996	10.4245	10.4270	10.4620	10.4670	10.4250	10.4580
2 1D_2	$\eta_{b2}(2D)$		10.3996	10.4244	10.4290	10.4650	10.4750	10.4320	10.4470
3 3D_3	$\Upsilon_3(3D)$		10.6383	10.6684	10.6790	10.7410	10.7400	–	–
3 3D_2	$\Upsilon_2(3D)$		10.6383	10.6684	10.6740	10.7400	10.7440	–	–
3 3D_1	$\Upsilon_1(3D)$		10.6383	10.6684	10.6660	10.7360	10.7420	–	–
3 1D_2	$\eta_{b2}(3D)$		10.6383	10.6683	10.6690	10.7400	10.7420	–	–
χ^2			0.0010	0.0005	0.0002				



(a) The hyperfine splitting of S states.

(b) The hyperfine splitting of P states.

Figure 3. The theoretical and experimental mass hyperfine splitting behavior of S and P states versus n

Also, in the experimental data, $n^3P_1 - n^3P_0; n = 1, 2$ is the dominant partial splitting. So, these expectations are consistent with practical results, as appear in Figs. 4 and 5. And we have presented our predictions for these states and the rest of the states, as in Table 4.

Table 3. Theoretical hyperfine splitting (Theo. $\Delta M_{Hyp.Sp.}$) and Experimental hyperfine splitting (Exp. $\Delta M_{Hyp.Sp.}$) of $[b\bar{b}]$ states in MeV for S, P, D-Wave studied states.

(n)	Wave Level (L)	Total Spin of states (S)	Hyperfine Splitting	Theoretical $ \Delta M_{Hyp.Sp} $	Experimental $ \Delta M_{Hyp.Sp} $ [43]
1	S	1-0	$^3S_1-^1S_0$	60	61.60
2	S	1-0	$^3S_1-^1S_0$	18	24.30
3	S	1-0	$^3S_1-^1S_0$	12	-
4	S	1-0	$^3S_1-^1S_0$	10	-
1	P	1-0	$^3P_1-^1P_1$	14	6.50
2	P	1-0	$^3P_1-^1P_1$	11	4.30
3	P	1-0	$^3P_1-^1P_1$	9	-
4	P	1-0	$^3P_1-^1P_1$	9	-
1	D	1-0	$^3D_2-^1D_2$	5	-
2	D	1-0	$^3D_2-^1D_2$	5	-
3	D	1-0	$^3D_2-^1D_2$	5	-

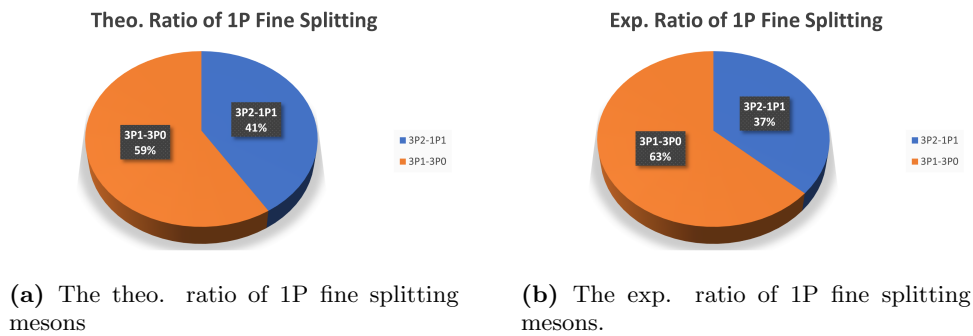


Figure 4. The theoretical and experimental fine splitting behavior of one spin 1P bottomonium states

4. CONCLUSION

In this work, we propose applying the three potentials in the framework of the non-relativistic quark model to probe the bottomonia spectra and obtain accurate yields. Our perspective depends on the non-relativistic framework that is suitable generally for the heavy mesons sector and particularly for bottomonium mesons because they are the heaviest mesons. The expectations of all these potentials present overall agree with practical data and with the theoretical expectations of other groups. The first one involves the one-gluon exchange interaction (like color coulomb potential) in addition to the scalar linear confinement potential, which provides us sensible findings where its uncertainty almost equals 0.0010, but it blinds concerning splitting between the multiples of bottomonium states which have the different S, and the J, but the same L quantum numbers. When we add the spin-spin interactions of quarks, we obtain the second potential, which is more accurate than the first one. Its χ value almost equals 0.005 and also exhibits hyperfine splitting behavior.

The third potential achieves our computational strategy that aims towards more accurate outputs using sophisticated treatments concerning the bottomonia spectrum, and we can extend and apply it to other heavy mesons. This potential is the most complex, but it is the most accurate one, with a χ value is almost 0.002. Additionally, it indicates the fine splitting behavior for bottomonium spectra. Our expected masses of unseen

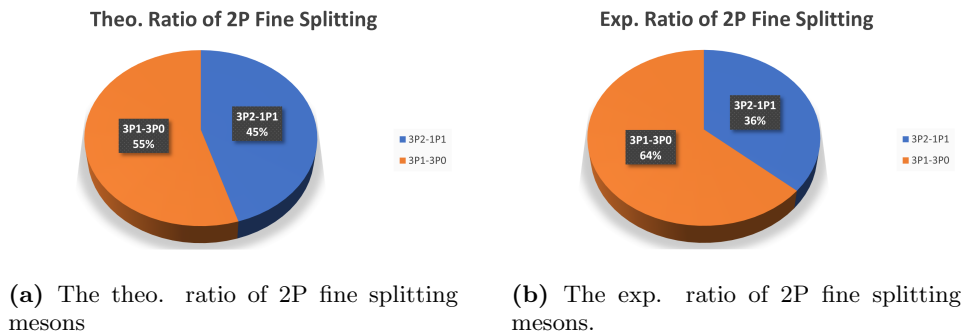


Figure 5. The theoretical and experimental fine splitting behavior of one spin 2P bottomonium states

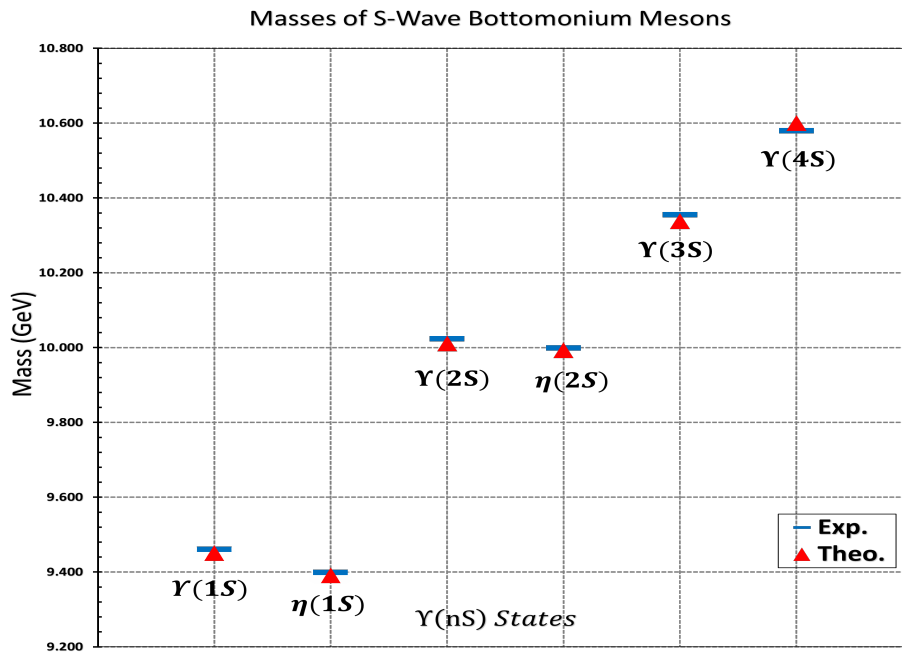


Figure 6. Comparing of the masses of S-wave bottomonia in GeV with the last update experimental data

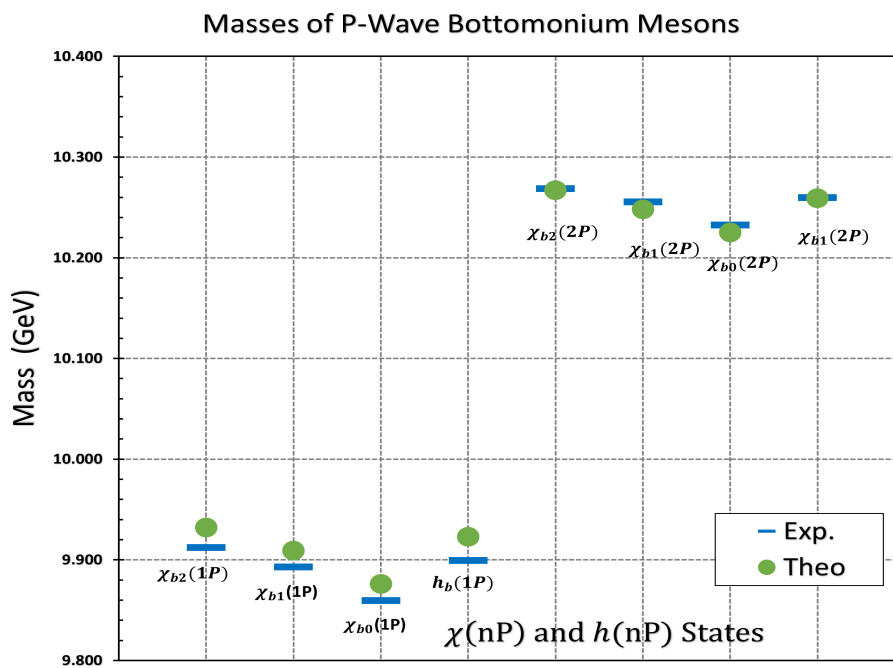


Figure 7. Comparing of the masses of P-wave bottomonia in GeV with the last update experimental data





Table 4. Theoretical fine splitting (Theo. $\Delta M_{F.Sp.}$) and Experimental fine splitting (Exp. $\Delta M_{F.Sp.}$) of $[b\bar{b}]$ states in MeV for P, D-Wave studied states.

n	Wave Level L	Total angular momentum of states (J)	Fine Splitting	Theo. $\Delta M_{F.Sp.}$	Exp. $\Delta M_{F.Sp.}$ [43]
1	P	2-1	3P_2 - 3P_1	23	19.4
	P	1-0	3P_1 - 3P_0	33	33.4
2	P	2-1	3P_2 - 3P_1	19	13.2
	P	1-0	3P_1 - 3P_0	23	23.0
3	P	2-1	3P_2 - 3P_1	17	-
	P	1-0	3P_1 - 3P_0	19	-
4	P	2-1	3P_2 - 3P_1	17	-
	P	1-0	3P_1 - 3P_0	16	-
1	D	3-2	3D_3 - 3D_2	5	-
	D	2-1	3D_2 - 3D_1	7	-
2	D	3-2	3D_3 - 3D_2	6	-
	D	2-1	3D_2 - 3D_1	7	-
3	D	3-2	3D_3 - 3D_2	5	-
	D	2-1	3D_2 - 3D_1	8	-

bottomonia states, via the third model, can provide good benefits to discovering these states in the incoming experiments.

So we use the yieldings from the third potential to study the hyperfine splitting behavior and the fine splitting behavior of the S, P, and D-wave bottomonia spectrum. This study of the bottomonia multiples behaviors agrees with the experimental data and presents significant predictions; we can use them to observe unseen bottomonium states in the future.

ORCID

 Moustafa Ismail Hapareer, <https://orcid.org/0000-0002-7654-6099>;  M. Allosh, <https://orcid.org/0000-0001-8389-7076>;  G.S. Hassan, <https://orcid.org/0000-0002-4830-0809>;  A.M. Yasser, <https://orcid.org/0000-0002-5891-1953>

REFERENCES

- [1] D. Griffiths, *Introduction to Elementary Particles*, (John Wiley, and Sons, Weinheim, 2020).
- [2] A. Bettini, *Introduction to Elementary Particle Physics*, Cambridge University Press, 2014.
- [3] F. Hanzel and A. D. Martin, *Quarks and leptons: An introductory course in modern particle physics*, (John Wiley, and Sons, New York, 1984).
- [4] D.H. Perkins, and D.H. Perkins, *Introduction to high energy physics*. (Cambridge university press, 2000). <https://doi.org/10.1017/CBO9780511809040>
- [5] I. Bigi, Y. Dokshitzer, V. Khoze, J. Kühn, and P. Zerwas, *Physics Letters B*, **181**(1-2), 157-163 (1986). [https://doi.org/10.1016/0370-2693\(86\)91275-X](https://doi.org/10.1016/0370-2693(86)91275-X)
- [6] S. Herb, D. Hom, L. Lederman, J. Sens, H. Snyder, J. Yoh, J. Appel, B. Brown, C. Brown, W. Innes, *et al.*, "Physical Review Letters, **39**(5), 252 (1977). <https://doi.org/10.1103/PhysRevLett.39.252>
- [7] W. R. Innes, J. Appel, B. Brown, C. Brown, K. Ueno, T. Yamanouchi, S. Herb, D. Hom, L. Lederman, J. Sens, *et al.* *Physical Review Letters*, **39**(20), 1240 (1977). <https://doi.org/10.1103/PhysRevLett.39.1240>
- [8] D. Besson, J. Green, R. Namjoshi, F. Sannes, P. Skubic, A. Snyder, R. Stone, A. Chen, M. Goldberg, N. Horwitz, *et al.* *Physical Review Letters*, **54**(5), 381 (1985). <https://doi.org/10.1103/PhysRevLett.54.381>
- [9] B. Aubert, M. Bona, Y. Karyotakis, J. Lees, V. Poireau, E. Prencipe, X. Prudent, V. Tisserand, J. G. Tico, E. Grauges, *et al.* *Physical Review Letters*, **101**(7), 071801 (2008). <https://doi.org/10.1103/PhysRevLett.101.071801>
- [10] R. Mizuk, D. Asner, A. Bondar, T. Pedlar, I. Adachi, H. Aihara, K. Arinstein, V. Aulchenko, T. Aushev, T. Aziz, *et al.* *Physical Review Letters*, **109**(23), 232002 (2012). <https://doi.org/10.1103/PhysRevLett.109.232002>
- [11] K. Han, T. Böhringer, P. Franzini, G. Mageras, D. Peterson, E. Rice, J. Yoh, J. Horstkotte, C. Klopfenstein, J. Lee-Franzini, *et al.* *Physical Review Letters*, **49**(22), 1612 (1982). <https://doi.org/10.1103/PhysRevLett.49.1612>
- [12] G. Eigen, G. Blamar, and H. Dietl "Evidence for χ_b ' *Physical Review Letters*, **49**(22), 1616 (1982). <https://doi.org/10.1103/PhysRevLett.49.1616>
- [13] C. Klopfenstein, J. Horstkotte, J. Lee-Franzini, R. Schamberger, M. Sivertz, L. Spencer, P. Tuts, P. Franzini, K. Han, E. Rice, *et al.* *Physical Review Letters*, **51**(3), 160 (1983). <https://doi.org/10.1103/PhysRevLett.51.160>
- [14] F. Pauss, H. Dietl, G. Eigen, E. Lorenz, G. Mageras, H. Vogel, P. Franzini, K. Han, D. Peterson, E. Rice, *et al.* *Physics Letters B*, **130**(6), 439 (1983). [https://doi.org/10.1016/0370-2693\(83\)91539-3](https://doi.org/10.1016/0370-2693(83)91539-3)

- [15] J. Lees, V. Poireau, E. Prencipe, V. Tisserand, J. G. Tico, E. Grauges, M. Martinelli, D. Milanese, A. Palano, M. Pappagallo, *et al.* *Physical Review D*, **84**(9), 091101 (2011). <https://doi.org/10.1103/PhysRevD.84.091101>
- [16] I. Adachi, H. Aihara, K. Arinstein, D. M. Asner, T. Aushev, T. Aziz, A. Bakich, E. Barberio, K. Belous, V. Bhardwaj, *et al.* *Physical Review Letters*, **108**(3), 032001 (2012). <https://doi.org/10.1103/PhysRevLett.108.032001>
- [17] P. del Amo Sanchez, J. Lees, V. Poireau, E. Prencipe, V. Tisserand, J. G. Tico, E. Grauges, M. Martinelli, A. Palano, M. Pappagallo, *et al.* *Physical Review D*, **82**(11), 111102 (2010). <https://doi.org/10.1103/PhysRevD.82.111102>
- [18] T. Kuhr, C. Pulvermacher, M. Ritter, T. Hauth, and N. Braun, *Computing and Software for Big Science*, **3**, 1 (2019). <https://doi.org/10.1007/s41781-018-0017-9>
- [19] Z.-G. Wang, *The European Physical Journal C*, **73**, 1 (2013). <https://doi.org/10.1140/epjc/s10052-013-2559-7>
- [20] K. Azizi and J. Söngü, *Journal of Physics G: Nuclear and Particle Physics*, **46**(3), 035001 (2019). <https://doi.org/10.1088/1361-6471/aace21>
- [21] C.S. Fischer, S. Kubrak, and R. Williams, *The European Physical Journal A*, **51**(1), 10 (2015). <https://doi.org/10.1140/epja/i2015-15010-7>
- [22] D.-M. Li, B. Ma, Y.-X. Li, Q.-K. Yao, and H. Yu, *The European Physical Journal C-Particles and Fields*, **37**, 323 (2004). <https://doi.org/10.1140/epjc/s2004-02002-5>
- [23] S. Gershtein, A. Likhoded, and A. Luchinsky, *Physical Review D*, **74**(1), 016002 (2006). <https://doi.org/10.1103/PhysRevD.74.016002>
- [24] K.-W. Wei, X.-H. Guo, *et al.* *Physical Review D*, **81**(7), 076005, (2010). <https://doi.org/10.1103/PhysRevD.81.076005>
- [25] A. Badalian and B. Bakker, *Physical Review D*, **100**(5), 054036 (2019). <https://doi.org/10.1103/PhysRevD.100.054036>
- [26] Y. Kiyo, and Y. Sumino, *Physics Letters B*, **730**, 76 (2014). <https://doi.org/10.1016/j.physletb.2014.01.030>
- [27] J. Daldrop, C. Davies, R. Dowdall, H. Collaboration, *et al.* *Physical Review Letters*, **108**(10), 102003 (2012). <https://doi.org/10.1103/PhysRevLett.108.102003>
- [28] R. Lewis and R. Woloshyn, *Physical Review D*, **85**(11), 114509 (2012). <https://doi.org/10.1103/PhysRevD.85.114509>
- [29] M. Wurtz, R. Lewis, and R. Woloshyn, *Physical Review D*, **92**(5), 054504 (2015). <https://doi.org/10.1103/PhysRevD.92.054504>
- [30] E. Van Beveren, G. Rupp, T. Rijken, and C. Dullemond, *Physical Review D*, **27**(7), 1527 (1983). <https://doi.org/10.1103/PhysRevD.27.1527>
- [31] N. Törnqvist *Physical Review Letters*, **53**(9), 878 (1984). <https://doi.org/10.1103/PhysRevLett.53.878>
- [32] J.-F. Liu and G.-J. Ding, *The European Physical Journal C*, **7253**(1), 18 (2012). <https://doi.org/10.1140/epjc/s10052-011-1853-5>
- [33] Y. Lu, M. N. Anwar, and B.-S. Zou, *Physical Review D*, **94**(3), 034021 (2016). <https://doi.org/10.1103/PhysRevD.94.034021>
- [34] D. Ebert, R. N. Faustov, and V. O. Galkin *The European Physical Journal C*, **71**, 1825 (2011). <https://doi.org/10.1140/epjc/s10052-011-1825-9>
- [35] M. Bhat, A. P. Monteiro, and K. Kumar, <https://doi.org/10.48550/arXiv.1702.06774>
- [36] S. Godfrey and N. Isgur *Physical Review D*, **32**(1), 189 (1985). <https://doi.org/10.1103/PhysRevD.32.189>
- [37] S. Godfrey and K. Moats *Physical Review D*, **92**(5), 054034 (2015). <https://doi.org/10.1103/PhysRevD.92.054034>
- [38] J.-Z. Wang, Z.-F. Sun, X. Liu, and T. Matsuki *The European Physical Journal C*, **78**, 915 (2018). <https://doi.org/10.1140/epjc/s10052-018-6372-1>
- [39] S. N. Gupta, S. F. Radford, and W. W. Repko *Physical Review D*, **34**(1), 201 (1986). <https://doi.org/10.1103/PhysRevD.34.201>
- [40] A. Badalian, A. Veselov, and B. Bakker, *Physical Review D*, **70**(1), 016007 (2004). <https://doi.org/10.1103/PhysRevD.70.016007>
- [41] M. Shah, A. Parmar, and P. Vinodkumar *Physical Review D*, **86**(3), 034015 (2012). <https://doi.org/10.1103/PhysRevD.86.034015>
- [42] C. Semay and B. Silvestre-Brac *Nuclear Physics A*, **618**(4), 455 (1997). [https://doi.org/10.1016/S0375-9474\(97\)00060-2](https://doi.org/10.1016/S0375-9474(97)00060-2)
- [43] R.L. Workman, *et al.*, “Review of Particle Physics,” *PTEP*, **2022**, 083C01 (2022). <https://doi.org/10.1093/ptep/ptac097>
- [44] J.-E. Augustin, A. Boyarski, M. Breidenbach, F. Bulos, J. Dakin, G. Feldman, G. Fischer, *et al.*, *Physical Review Letters*, **34**(4), 233 (1975). <https://doi.org/10.1103/PhysRevLett.34.233>
- [45] T. Appelquist, A. De Rujula, S.L. Glashow, and H. Plitzer, *tech. rep.*, SIS-75-0111, 1974
- [46] A. De Rujula, and S.L. Glashow, *Physical Review Letters*, **34**(1), 46 (1975). <https://doi.org/10.1103/PhysRevLett.34.46>

- [47] A.A. Bykov, I.M. Dremin, and A.V. Leonidov, *Soviet Physics Uspekhi*, **27**(5), 321 (1984)
- [48] T. Barnes, S. Godfrey, and E. Swanson, *Physical Review D*, **72**(5), 054026 (2005).
<https://doi.org/10.1103/PhysRevD.72.054026>
- [49] B.L. Ioffe, V.S. Fadin, and L.N. Lipatov, *Quantum chromodynamics: Perturbative and nonperturbative aspects*. No. 30, (Cambridge University Press, 2010).
- [50] O. Lakhina, PhD thesis, University of Pittsburgh, 2007
- [51] A. Yasser, T. Nahool, and G. Hassan, (2014). <https://doi.org/10.48550/arXiv.1410.5005v>
- [52] L. Bai-Qing and C. Kuang-Ta, *Communications in Theoretical Physics*, **52**(4), 653 (2009).
<https://doi.org/10.1088/0253-6102/52/4/20>
- [53] I. Asghar, F. Akram, B. Masud, and M.A. Sultan, *Physical Review D*, **100**(9), 096002 (2019).
<https://doi.org/10.1103/PhysRevD.100.096002>
- [54] V. Kher, R. Chaturvedi, N. Devlani, and A. Rai, *The European Physical Journal Plus*, **137**(3), 357 (2022).
<https://doi.org/10.1140/epjp/s13360-022-02538-5>
- [55] B. Chen, A. Zhang, and J. He, *Physical Review D*, **101**(1), 014020 (2020).
<https://doi.org/10.1103/PhysRevD.101.014020>
- [56] W.-J. Deng, H. Liu, L.-C. Gui, and X.-H. Zhong, *Physical Review D*, **95**(7), 074002 (2017).
<https://doi.org/10.1103/PhysRevD.95.074002>

БОТОМОНІЯ ПІД ВПЛИВОМ ТРЬОХ ІНСПІРОВАНИХ ПОТЕНЦІАЛІВ КХД У РАМКАХ НЕРЕЛЯТИВІСТСЬКОЇ КВАРКОВОЇ МОДЕЛІ

Мустафа Ісмаїл Хапарір,^a М. Аллош^b, Г.С. Хассан^a, А.М. Ясер^b

^aКафедра фізики, Факультет природничих наук, Асьют, Університет Асьют, 71515 Асьют, Єгипет

^bФізичний факультет, природничий факультет, Кена, Університет Південної долини, 83523 Кена, Єгипет

У цій статті ми досліджували спектр поведінки боттонієвих мезонів під впливом трьох типів потенціалів, навіяних квантовою хромодинамікою. Крім того, були вивчені інші властивості, такі як поведінка гіпертонкого розщеплення та поведінка тонкого розщеплення. Ми використали ці потенційні моделі в рамках моделі нерелятивістських кварків, щоб представити це дослідження. Ми виявили, що наші очікування узгоджуються з експериментальними даними та іншими теоретичними роботами, а також ми представили нові висновки щодо спектру невидимих станів боттомонію для S, P і D-хвиль боттомонії. І ми очікували інших їхніх характеристик.

Ключові слова: властивості гіперрозщеплення; тонке розщеплення; боттомонія